Feasibility of Seasonal Forecasts Inferred from Multiple GCM Simulations

W. STERN AND K. MIYAKODA

Geophysical Fluid Dynamics Laboratory/NOAA, Princeton University, Princeton, New Jersey

(Manuscript received 26 October 1993, in final form 22 September 1994)

ABSTRACT

Assuming that SST provides the major lower boundary forcing for the atmosphere, observed SSTs are prescribed for an ensemble of atmospheric general circulation model (GCM) simulations. The ensemble consists of 9 "decadal" runs with different initial conditions chosen between 1 January 1979 and 1 January 1981 and integrated about 10 years. The main objective is to explore the feasibility of seasonal forecasts using GCMs. The extent to which the individual members of the ensemble reproduce the solutions of each other (i.e., reproducibility) may be taken as an indication of potential predictability. In addition, the ability of a particular GCM to produce realistic solutions, when compared with observations, must also be addressed as part of the predictability problem.

A measure of reproducibility may be assessed from the spread among ensemble members. A normalized spread index, σ_n/σ_s, can be defined at any point in space and time, as the variability of the ensemble (σ_n) normalized by the climatological seasonal variability (σ_s). In the time mean it is found that the reproducibility is significantly below unity for certain regions. Low values of the spread index are seen generally in the Tropics, whereas the extratropics does not exhibit a high degree of reproducibility. However, if one examines plots in time of seasonal mean σ_n/σ_s for the U.S. region, for example, it is found that for certain periods this index is much less than unity, perhaps implying "occasional potential predictability." In this regard, time series of ensemble mean soil moisture and precipitation over the United States are compared with corresponding observations. This study reveals some marginal skill in simulating periods of drought and excessive wetness over the United States during the 1980s (i.e., the droughts of 1981 and 1988 and the excessive wetness during the 1982/83 El Niño). In addition, by focusing on regions of better time-averaged reproducibility—that is, the southeast United States and northeast Brazil—a clearer indication of a relationship between good reproducibility and seasonal predictability seems to emerge.

1. Introduction

The ability to predict significantly anomalous and persistent weather regimes, such as droughts and extended cold waves, would no doubt have very positive socioeconomic impact. The primary objective of this study is to explore the feasibility of seasonal prediction of atmospheric states with a GCM, the ultimate goal being predictions on the timescale of one to ~ three seasons.

On the timescale of 1 month it has been shown that some large-scale quasi-stationary anomalous circulation features could be successfully predicted from initial conditions, without specifying anomalous boundary conditions (Miyakoda et al. 1983). As the length of predictions extend beyond a month, the focus of the problem should be more on boundary conditions than the atmospheric initial conditions (Shukla 1985). For predictions of one season and beyond, it is rather unlikely that predictability decay would allow much information from the initial conditions to be retained. Hence, it seems that the presence of systematic external forcing is crucial for predictive skill on the seasonal timescale. It is assumed that sea surface temperatures (SST) provide the major component of external forcing to the atmosphere.

There are numerous studies of the effects of SST, particularly related to the El Niño/Southern Oscillation (ENSO), including extended range prediction studies at the Geophysical Fluid Dynamics Laboratory (GFDL), since 1966. Among the variety of topics on this subject, this paper focuses on model simulations with specified SST fields. This is not a forecasting study per se, since SSTs are not being predicted. However, these experiments may be viewed as a preliminary prerequisite study toward seasonal prediction, which eventually should be performed with coupled models (Miyakoda et al. 1993).

Long period simulations based on uncoupled models have been performed previously. In particular, Lau (1985) conducted a 15-yr simulation (1962–76) using observed month-to-month SST over the tropical Pacific. He investigated the recurrent patterns of global atmospheric circulation. Subsequently there have been a number of papers published along this line. Limiting references to those involving long-term (more than 10 yr) integrations with observed SST globally (60°N

Corresponding author address: William Stern, Geophysical Fluid Dynamics Laboratory, Princeton University, Forrestal Campus, US Route 1, P.O. Box 308, Princeton, NJ 08542.

~ 40°S) specified, quite a few studies have already appeared in the literature as listed in Table 1.

These papers in Table 1 (and others investigating SST impact) touch on various topics, including the ENSO process (Rasmusson and Carpenter 1982), the global effect of the ENSO phenomena (e.g., Rowntree 1972; Horel and Wallace 1981; van Loon and Rogers 1981), recurrent teleconnection patterns (Wallace and Gutzler 1981), and teleconnection processes (Hoskins and Karoly 1981; Simmons et al. 1983). All these topics are relevant to the study in this article.

Although it is not explicit, there is another topic of concern here, that is, the nonlinear processes associated with instabilities or "nonlinear dynamics," in which even small perturbations in initial conditions will produce substantially different solutions (and as a consequence may create a myriad of bifurcations) (e.g., Pitcher et al. 1988; Navarra and Miyakoda 1988; Kushnir and Lau 1992; Ting and Held 1990). Therefore, "predictability" on the seasonal timescale requires the ensemble concept, in which multiple realizations are involved.

The focus of the present paper is decadal timescale model simulations with observed SST prescribed. The paper's main contribution is to discuss the feasibility of seasonal prediction based on the behavior of an ensemble of simulations.

A description of the model and experiments is provided in section 2. The main results are based on a version of the model using a spectral triangular truncation at wave 30 (T30) and having 18 vertical levels (L18), T30L18 (hereafter referred to as "T30SM"—see Stern and Miyakoda 1991). Since the quality of the atmospheric model may affect the validity of some of the conclusions, the model is compared with observations, by looking at some seasonal mean and interannual general circulation statistics in section 3. In section 4 the spread among ensemble members is investigated. Section 5 looks at reproducibility and how it may relate to seasonal prediction capability, including a validation of the model's seasonal predictions of anomalous wet and dry episodes. Finally a summary of key results and conclusions are presented in section 6, followed by a discussion regarding the problems of initial soil moisture specification in the appendix.

TABLE 1. Studies involving long-term model integrations with observed SST globally specified.

Authors	SST specified (yr)	Duration	Model resolution	Atmospheric response examined
Latif et al. (1990)	16	(1961–85)	T21L19	Tropics
Kitoh (1991a)	21	(1969–90)	5° × 4°L5	Tropics
Lau and Nath (1990)	30	(1950–79)	R15L9	Extratropics
Kitoh (1991b)	the same as Kitoh (1991a)			Extratropics
König and Kirk (1991)	19	(1970–88)	T21L19	Extratropics
Ponater and König (1991)	the same as above			Extratropics

Note: T21, R15, or 5° × 4° indicates model's horizontal resolution, where "T" and "R" denote triangular and rhomboidal truncation, respectively. L19, L9, or L5 indicate number of vertical levels.

2. Experimental design

The model used in this study is a global atmospheric spectral GCM; the basic model is described in Gordon and Stern (1974; 1982). As indicated in section 1, the primary version used in these experiments was the T30SM. The major physical parameterizations include a "bucket" hydrology; orographic gravity wave drag (Stern and Pierrehumbert 1988); large-scale condensation and moist convective adjustment (both using a condensation criteria of 100%); shallow convection; cloud prediction (interactive with the radiation, Gordon 1992); radiative transfer (12 h averaged) that varies seasonally; stability dependent vertical eddy fluxes of heat, momentum and moisture throughout the surface layer, planetary boundary layer and free atmosphere ("E" physics as described in Sirutis and Miyakoda 1990); and $k\nabla^4$ horizontal diffusion. This model with simpler physics and varying resolutions has been shown to be viable for numerical weather prediction at the monthly timescale (Stern and Miyakoda 1989), although systematic biases still contribute significantly to the error fields.

The main focus of this paper will be the results of nine multiyear model integrations with the T30SM described above. A preliminary study was presented in Stern and Miyakoda (1991). Initial conditions were chosen between 1 January 1979 and 1 January 1981, spaced three months apart. All cases were run through 31 December 1988 with the same observed sea surface temperatures (SSTs) specified (Reynolds 1988). Some reference will occasionally be made to a later set of experiments that used a T42L18 version of the same atmospheric spectral GCM (hereafter referred to as T42SM) and *a revised observed SST dataset* used in AMIP (the atmospheric model intercomparison project) (Gates 1992). This second ensemble experiment also consists of nine multiyear integrations, but in this case all initial conditions were taken as 1 January 1979 (i.e., the nine initial conditions were taken from analyses between 12 December 1978 and 21 January 1979 spaced 5 days apart and treating these as independent estimates of the initial state on 1 January 1979).

The concept of using a global SST dataset as boundary forcing for the atmosphere was advocated by Namias (1986) and has been used in other GOGA (Global Ocean Global Atmosphere) GCM experiments, such as, Lau and Nath (1990) and König and Kirk (1991) (though they called it GAGO). The unique aspects of this study are the generation of an ensemble of GCM integrations to examine reproducibility among the en-

semble members and proposing that reproducibility may be related to potential predictability.

Specification of land surface conditions has not been mentioned thus far. It has been assumed that SSTs provide the major component of external forcing to the atmosphere. Is proper land surface boundary information (i.e., soil moisture) also necessary? One can make the argument that SST anomalies will drive soil moisture anomalies if SST anomalies are associated with atmospheric circulation patterns. For the current study involving multiyear integrations, it is assumed that there is sufficient time for land surface fields to fully respond to SST forcing, hence, their initial specification is not crucial. However, this may not be the case for a single season prediction, since the response time for the land surface fields could be as long or longer than the forecast. Some related discussion is included in the appendix.

3. Validation of the model

Although it is not at all obvious what qualifications make a GCM suitable for a feasibility study of seasonal prediction, it seems reasonable to expect some degree of realism in its ability to simulate general circulation statistics. The specific focus here is to look at the simulation of seasonal means and interannual variability in the T30SM and compare them with available observations.

a. Climatological means (first moment quantities)

Seasonal model climatologies have been calculated based on an average of the respective seasons from each simulated model year (excluding the first year, i.e., 1979) as follows:

Assume that x is a time series of a seasonal mean variable, $x_{\eta,y}$. Here $x_{\eta,y}$ represents the ηth member among an ensemble of size N for the yth year of a simulation of length Y.

The average of the first kind is the ensemble mean; that is,

$$\langle x \rangle_y = \frac{1}{N} \sum_{\eta=1}^{N} x_{\eta,y}, \tag{3.1}$$

where $N = 9$ members for the experiments described in this paper.

Therefore, $\langle x \rangle_y$ is a function of y, where y ranges from 1 to Y.

Another average is taken with respect to years; that is,

$$\bar{x}_\eta = \frac{1}{Y} \sum_{y=1}^{Y} x_{\eta,y}, \tag{3.2}$$

where $Y = 9$ years for those cases starting in 1979 (i.e., 1980–88), and $Y = 8$ for those starting on or after 1 January 1980 (i.e., 1981–88). Therefore, $\bar{x}_\eta$ is a function of η, where $\eta = 1, 2 \cdots N$.

Applying both averages to x, yields

$$\overline{\langle x \rangle} = \frac{1}{N \cdot Y} \sum_{y=1}^{Y} \sum_{\eta=1}^{N} x_{\eta,y}, \tag{3.3}$$

the ensemble mean as well as interannual average over Y years, and, therefore, $\langle x \rangle$ (climatological mean) is a function of season.

For validation of the model's seasonal mean general circulation, an 8-year average (1980–87) of European Centre for Medium-Range Weather Forecasts (ECMWF) analyses as processed by Schubert et al. (1990) was used (hereafter referred to as OBS).

Most of the discussion of the T30SM's ability to simulate seasonal mean circulation features will focus on zonal wind (U) at 200 hPa and precipitation rate. These particular quantities were chosen to give an indication of the model's ability to simulate the jet flow and to look at the climatology of a field that is of great interest for seasonal prediction, that is, precipitation rate. First, however, a few comments about the zonal-mean latitude–height distribution of U (not shown) seem appropriate. There is overall agreement with OBS in the latitudinal and vertical positioning of the jet maxima in both hemispheres for both boreal winter (DJF—December-January-February) and summer (JJA). The magnitude of the Northern Hemisphere winter jet maximum is too weak in the T30SM when compared with OBS, while the summer maximum is somewhat strong. In the Southern Hemisphere there is excellent agreement between the model and OBS for the magnitude of the JJA jet maximum, while the model's DJF maximum is somewhat strong. One of the largest disagreements between the T30SM and OBS for zonal mean U, occurs in the upper equatorial troposphere centered around 300 hPa. Here the model shows a significant westerly bias.

1) U AT 200 hPa

Figure 1 shows the DJF climatological mean for U at 200 hPa. The T30SM is shown in the top panel and the OBS at the bottom. In general there is qualitative agreement, except for a spurious area of strong westerlies in the eastern equatorial Pacific around 120°W. As was indicated in the preceding discussion of zonal mean U, the Northern Hemisphere extratropical jet maxima are significantly weaker than OBS. The westerly bias in the equatorial, zonal-mean, upper-tropospheric U field can be seen here as weaker model easterlies over New Guinea and Borneo (in addition to the previously noted eastern equatorial Pacific westerly error).

2) PRECIPITATION RATE

Figure 2 compares climatological precipitation rate in the T30SM with the observed climatology produced

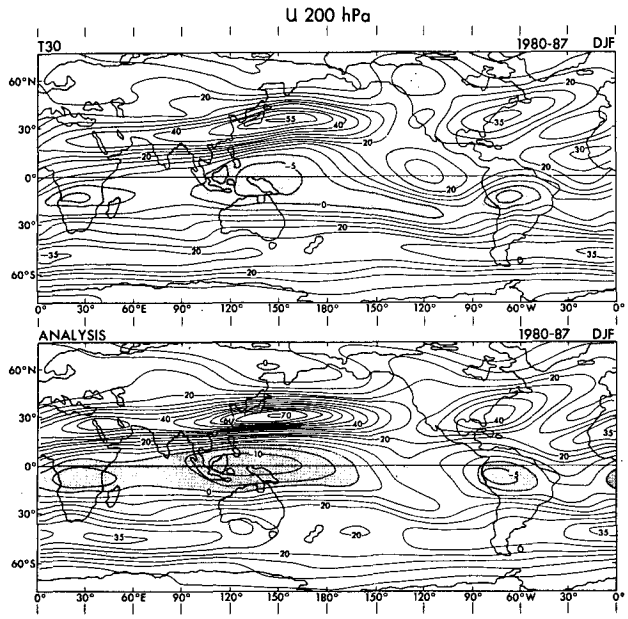

FIG. 1. Zonal component of wind, u, at 200-hPa level for DJF, averaged for 8-yr model simulation (*upper*) and the observational analysis (*lower*) compiled by Schubert et al. (1990). Contour interval is 5 m s^{-1}. Easterlies indicated with shading.

by Möller (1951). The general distribution of tropical rainfall shows reasonable agreement for both DJF and JJA. Particularly good agreement with observation is found for the large-scale precipitation pattern over the Indian subcontinent and for the distribution in JJA (not shown) along the intertropical convergence zone (ITCZ) over the Pacific.

For DJF the main deficiency of the model is in the excessive rainfall rates over the equatorial zone, that is, the South Pacific convergence zone (SPCZ), and over Brazil. The model orography appears to produce spuriously large amounts of rain in South America especially along the Andes. In this region the Gibbs error associated with truncation of steep orography (Navarra et al. 1994) is hypothesized to be the main cause of this spurious rainfall.

Further weaknesses to note in the DJF simulation involve dry areas and the ITCZ. The dry zones normally located off the west coast of continents are not well simulated as they do not extend sufficiently westward, particularly off Australia toward the South Indian Ocean. Finally, the ITCZ over the eastern Pacific and the Atlantic are not well reproduced.

In general the T30SM seems to broaden the precipitation associated with the ITCZ, when compared to observations, while zonally limiting low precipitation regions. A major weakness is an excessive enhancement of the ITCZ in JJA (not shown) in the western Pacific near the Philippines.

In the extratropics there is a disagreement with the Möller distribution of storm track precipitation. The model precipitation is significantly greater in magnitude and extent; however, in these regions there is speculation that the Möller data is an underestimate based on a more recent precipitation climatology (i.e., Legates and Willmott 1990).

b. Climatological variances (second moment quantities)

Climatologies of model variability have been calculated for each season as the variance of all ensemble members ($N = 9$) and all simulated model years ($Y = 9$), excluding the first year, that is, 1979; as follows:

$$\sigma_s^2 = \frac{1}{N \cdot Y} \sum_{y=1}^{Y} \sum_{\eta=1}^{N} x'^2_{\eta,y}, \tag{3.4}$$

where x' anomalies are defined as

$$x'_{\eta,y} = x_{\eta,y} - \overline{\langle x \rangle}, \tag{3.5}$$

where σ_s^2 is a function of time of year. In this paper the discussion of seasonal variability will focus on geopotential at 200 hPa.

Before looking at the details of geopotential at 200 hPa, some comments regarding variability of the prescribed SSTs seems appropriate. The variance of observed SST (Reynolds 1988) has been calculated, in a way similar to (3.4), with $N = 1$, and the square root σ_s, is taken. It is not shown here but is presented in König and Kirk (1991) (their figure is for January instead of DJF). Variance of SST for DJF has its largest values over the eastern equatorial Pacific and eastern

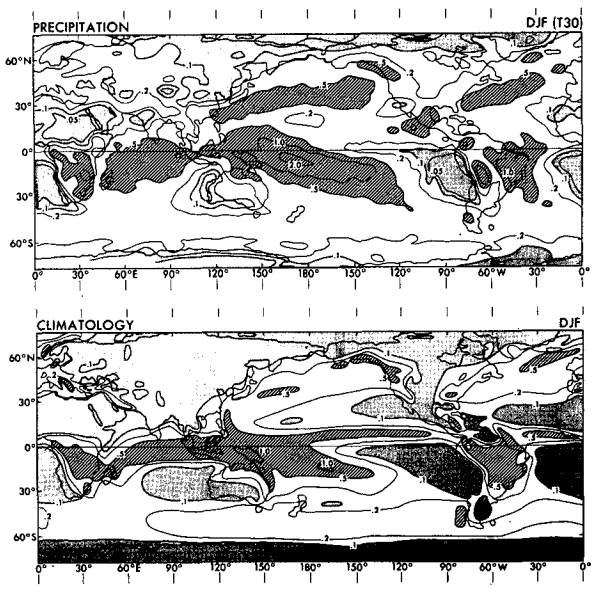

FIG. 2. Rate of precipitation for DJF, averaged for 9 years of model simulations (*upper*), and for the observed climatology (*lower*) compiled by Möller (1951). Contours are 1.0, 0.5, 0.2, 0.1, 0.05, and ~0 cm d^{-1}. Areas <0.1 cm d^{-1} are shaded and areas >0.5 cm d^{-1} are hatched.

equatorial Atlantic. It should be noted that the variance over the Gulf Stream and Kuroshio regions is not large. The variance for JJA (also not shown here) is similar to that of DJF.

Figure 3 shows a comparison of (DJF) σ_s for geopotential (Z) at 200 hPa between the T30SM ensemble (top) and NMC (National Meteorological Center) observations (bottom). Both model and observations are for the same 9-yr period (1980–88; i.e., $Y = 9$), but $N = 9$ for the T30SM while $N = 1$ for the observations.

The largest values of seasonal variability generally appear outside the Tropics in the mid- and high latitudes, although there is a relative maximum in the tropical eastern Pacific. There is some correspondence in positioning of variability centers between the T30SM and observations, especially in the east tropical Pacific and North Pacific regions. However, the observations have more distinct centers, and amplitudes of these centers in the model are significantly weaker than in the observations. Most aspects of the DJF comparison apply to JJA as well (not shown), although the reduction of amplitude in the model relative to observations is not as great in the Northern Hemisphere summer.

Lau and Nath (1990) calculated this same measure of height variability from 28 Northern Hemisphere winters of a single 30-yr simulation with prescribed SST (i.e., $Y = 28$, $N = 1$). Their results are shown (in their Fig. 16) for height at 515 hPa for the Northern Hemisphere poleward of 20°N and are qualitatively quite similar to those from the ensemble of T30SM simulations.

This underestimate of 200-hPa midlatitude variability in the T30SM when compared with the NMC observations, may be indicating a deficiency in wave activity propagating out of the Tropics. This might tend to worsen midlatitude reproducibility estimates (discussed in the next section).

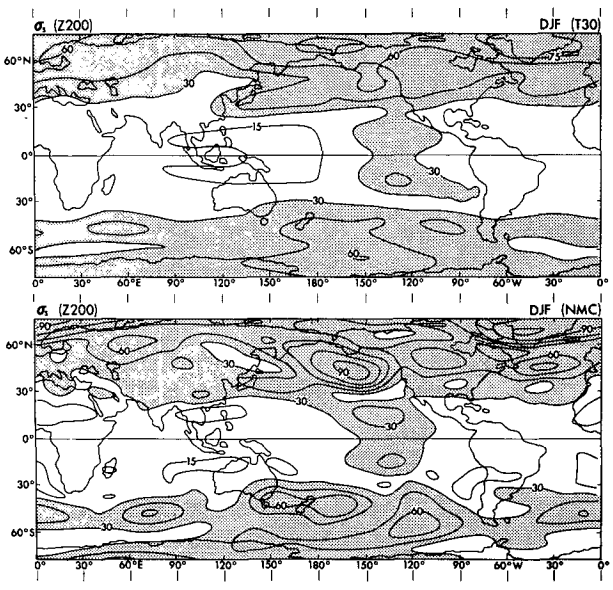

FIG. 3. Standard deviation of the geopotential height at 200 hPa for DJF, obtained by the model (upper) and for the observation (NMC analysis) (lower). Contour interval is 15 m.

c. *Response of the tropical atmosphere*

As noted earlier there have been numerous studies that show the importance of ENSO on both observed and model circulation features, particularly in the Tropics. Lau and Nath (1990) have indicated that prescribed SST fluctuations were much more effective in enhancing the amplitude of atmospheric (interannual) variability in the Tropics than in the extratropics. Hence, it seems crucial to establish that the T30SM responds reasonably to ENSO forcing in the Tropics. In this regard, the focus here will be on the interannual variation in time series of the Southern Oscillation index (SOI).

To assess the model's capability for simulation of the equatorial (Walker) circulation, time series of SOI (normalized surface pressure difference between Tahiti and Darwin) are examined by comparing with the observation. Figure 4 shows the SOI for model and observation. Both represent 5-month running averages; the model's results are based on the nine case ensemble mean, whereas the observation is, of course, one realization. Both the observed and the model have been calculated following the normalization procedure described by Troup (1967). However, the T30SM uses its own standard deviation, calculated from 1980 to 1988, whereas the observed standard deviations were based on data from 1951 to 1980. This difference in calculation periods for the normalizing standard deviations may explain the relative weakness of the model SOI as seen in Fig. 4.

The SOI based on the model simulations (as defined above) appears to underestimate the 1982/83 El Niño (some of this is probably due to the difference in normalization periods), with significant overestimates in 1981 and the 1984–85 periods. A close resemblance is also seen in results from the MRI (Meteorological Research Institute) GCM (Kitoh 1991a; Fig. 4). König and Kirk (1991) note similar errors in their SOI simulations and Latif et al. (1990) described their comparison as "the observed and the simulation are not well related to each other on time scales of a few months, but on time scales longer than a year they coincide," and "the intensity of the model's SOI is too weak." These comments seem appropriate here as well.

In the case of the simulation of the Southern Oscillation during the 1982/83 El Niño by the T30SM, it appears that the disagreement of surface pressure variation with observations is larger at Darwin than at Tahiti.

d. *Summary*

Overall features of the T30SM appear realistic. However, with the eventual goal of real time seasonal

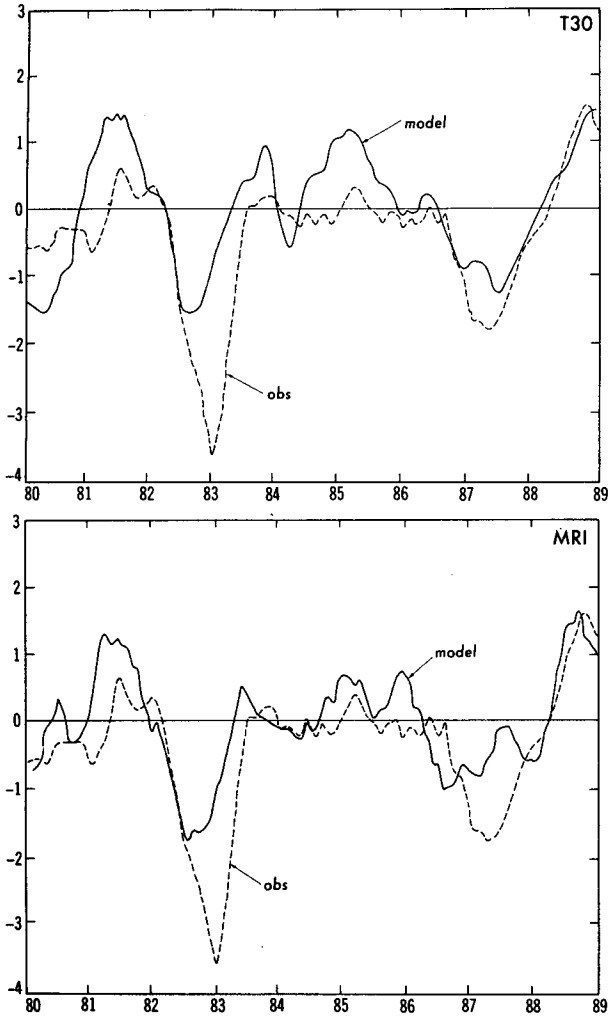

FIG. 4. Southern Oscillation index of the model (solid line) and observed (dashed line). T30 model in this study (upper), and Kitoh (1991a)—MRI model (lower).

prediction in mind (i.e., coupled ocean–atmosphere prediction), there is a need for a more critical evaluation. A higher standard of performance is needed because the air–sea coupling demands a high degree of accuracy in the near-ocean-surface simulation. In this regard, a major problem seen in the validation of the T30SM will be summarized below.

A number of errors discussed in subsection *a* appear to contribute to a deficiency in the T30SM's simulation of the Walker Circulation in the equatorial Pacific. The upper-tropospheric westerly errors across the central and eastern Pacific, coupled with the stronger model easterlies in the vicinity of India (especially for JJA) appear to be indicative of an updraft center in the western Pacific that is too strong (associated with the spuriously heavy precipitation in that region). Consistent with this scenario is the model's weak easterlies near the surface over New Guinea and Borneo, as well as, the previously noted errors in the surface wind stress along the SPCZ and ITCZ. It has been noted that much of the disagreement in the T30SM simulation of the SOI for 1982/83 can be traced to errors in the vicinity of Darwin. This gives an additional indication that the excessive condensation in the western equatorial Pacific may be a major contributor to distortions in the Walker Circulation. It is of interest, however, that a time evolution of model wind stress anomalies (i.e., the biases of the model climate have been removed) over the equatorial Pacific (not shown) are quite reasonable.

In earlier experiments using a version of the model similar to T30SM, the erroneous heavy rainfall in the western tropical Pacific did not appear, Sirutis and Miyakoda (1990) (see Fig. 18 Model E in that paper). The physics of the two model versions were close but not identical. From comparisons at this time it is speculated that the current implementation of the "shallow convection" parameterization (Tiedtke 1986) may be a candidate for the cause. This parameterization has proven beneficial in evicting excessive moisture from the surface layer, but given the current configuration of model physics some revisions to this scheme appear to be needed here.

4. Spread among the ensemble members

The fundamental issue of this paper is to attempt to assess the feasibility of seasonal prediction with a GCM. The approach here is to monitor the behavior of an ensemble prediction system, that is, determine whether the distribution of solutions of individual predictions within the ensemble shows some systematic or reproducible behavior or whether it is chaotic. Palmer (1993) presented an illustrative example of ensemble prediction using a simple three-component Lorenz convection model (Lorenz 1963). Using phase-space diagrams he showed various evolutions of ensembles of initial points on the Lorenz attractor and looked at their dispersion in time. In this study the dispersion or scatter of the members of the ensemble is referred to as the ensemble spread.

There is perhaps some question as to the size and characteristics of the initial ensemble. The choice of nine simulations here was dictated mainly by computational feasibility. In applying the ensemble approach to dynamical predictions of up to 30 days, there has been some concern about how to generate initial perturbations (Vukicevic 1991; Palmer 1993). In those situations predictability is very much a function of initial conditions, so being able to properly sample the uncertainty space associated with initial conditions is rather important. The simplicity in choice of the initial conditions used here may be justified by the timescale of the problem at hand. On the seasonal timescale, predictability is generally assumed not to be a function of initial state but rather a response of the atmosphere to boundary forcing.

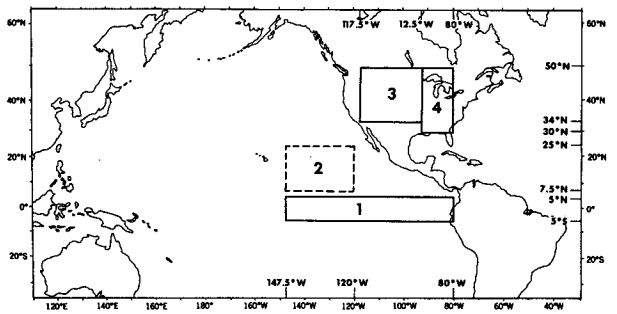

FIG. 5. Tropical and subtropical regions are indicated by 1 and 2, respectively, and U.S. response regions are noted by 3 and 4, respectively.

a. A measure of spread

Examples of the ensemble dispersion will be presented for precipitation rate as a function of time for geographical regions as indicated in Fig. 5,[1] that is, box 1 in the equatorial eastern Pacific, and boxes 3 and 4 combined over much of the United States. For this presentation and for validation of model seasonal simulations later, it is convenient to look at anomaly quantities—that is, climatology removed—as defined in (3.5).

It can be seen in Fig. 6 that the anomalies of precipitation rate from the nine simulations show considerable consistency for box 1 (upper panel). In other words, the model simulations are quite reproducible. However, for boxes 3 and 4 (lower panel) there is significant scatter among the ensemble solutions. This is apparently a consequence of the combined effect of various dynamical instabilities, particularly baroclinic eddies in the extratropics.

A quantitative measure of scatter among the multiple realizations may be defined as the standard deviation of a seasonal mean variable, x, over the ensemble of integrations; the squared quantity (variance) is calculated as follows:

$$\sigma_n^2 = \frac{1}{N} \sum_{\eta=1}^{N} (x_\eta - \langle x \rangle)^2, \tag{4.1}$$

where $N = 9$ and $\langle x \rangle$ is defined in Eq. (3.1), except "y" subscripts have been dropped.

b. Geographical distribution of reproducibility

Here, σ_n has seasonality, which can be removed if σ_n is divided by the model's (climatological) seasonal variability, σ_s, from (3.4). This ratio,

$$R = \frac{\sigma_n}{\sigma_s}, \tag{4.2}$$

is defined here as "reproducibility"—that is, the normalized standard deviation over multiple realizations or simply the normalized spread. Defined in this way, smaller values would indicate greater reproducibility.

The robustness of the geographical variability of R is enhanced by looking at its time average, $\bar{R}$. It is evident from Eqs. (3.4) and (4.1) that $\overline{R^2} = \overline{\sigma_n^2}/\sigma_s^2 \leq 1$ and, after some algebraic manipulation, that $\bar{R} \leq 1$.

A zonal average of this quantity (with I being the number of longitudes around a latitude),

$$\sum R = \frac{1}{I} \sum_{i=1}^{I} \bar{R}_i, \tag{4.3}$$

as a function of latitude is presented in Figs. 7 and 8 for various fields. In Fig. 7 selected variables are plotted for DJF: they are the precipitation rate, *PRC*; the zonal component of wind at 850 hPa, u850; and at 200 hPa, u200; the meridional component of wind at the 200-hPa level, v200; the temperature at 200 hPa, T200; and the geopotential heights at 200 hPa, z200 and 500 hPa, z500. The overall features in Fig. 7 are (a) reproducibility is best at the equator for almost all variables,

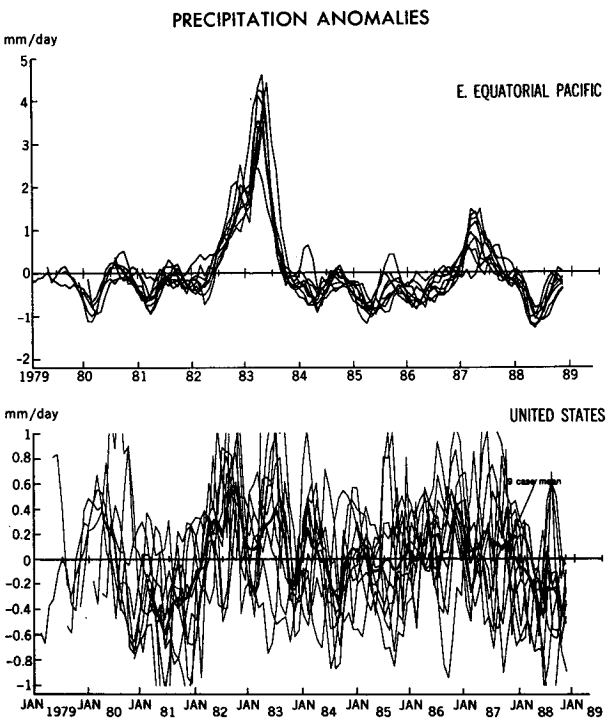

FIG. 6. Precipitation anomalies from each of the nine simulations, averaged over box 1—eastern equatorial Pacific region (upper), and over boxes 3 and 4 combined—east and west regions of the United States (lower).

[1] Motivation for adopting the boxes shown in Fig. 5 comes from the study of Trenberth et al. (1988), though Trenberth and Branstator (1992) further indicate that the total tropical SST anomaly pattern must be considered for understanding the causes of the 1988 U.S. drought.

and (b) z200, z500, u200, and T200 are better than v200, u850, and PRC, with PRC showing generally the least reproducibility. It is interesting to note the secondary minimum in PRC near 30°N, which corresponds to the approximate position of the subtropical jet. Figure 8 exhibits that better reproducibility extends toward higher latitudes (in both hemispheres) more in JJA than in DJF. Palmer (1994, personal communication) has suggested that reproducibility in the extratropics is influenced by two contrasting factors. The first is associated with teleconnections from the Tropics, which is assumed to increase reproducibility and is presumed to be largest in the winter. In contrast, the second factor, midlatitude internal variability, might tend to reduce reproducibility and is weakest in the summer. It is possible that the relative importance of these two factors is different in the two hemispheres. Figure 8 also includes the reproducibility of the temperature at 850 hPa, T850. These very low values of ΣR are consistent with the expected influence of the prescribed SSTs on T850 due to its close proximity.

In the early 1980s it was hypothesized by Shukla (1985) that the Tropics should be more predictable than the extratropics based on the large impact of the lower boundary in the Tropics seen in a model simulation. To the extent that reproducibility is an indicator of predictability, then the global distributions of σ_n/σ_s (R from 4.1) shown in Figs. 9 and 10 support Shukla's hypothesis. It is clear for both precipitation rate (Fig. 9) and Z500 (Fig. 10) that the best reproducibility is found in the equatorial region, particularly over the equatorial Pacific with secondary centers over the tropical Atlantic and Indian Oceans. It should be noted that the strength of the 82/83 El Niño is a major contributor to the excellent reproducibility seen in the eastern equatorial Pacific.

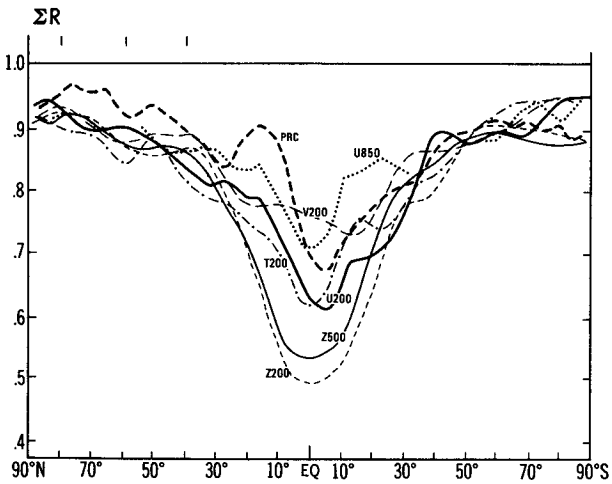

FIG. 7. Latitudinal distribution of zonally averaged reproducibility, ΣR from Eq. (4.3), for various variables during DJF.

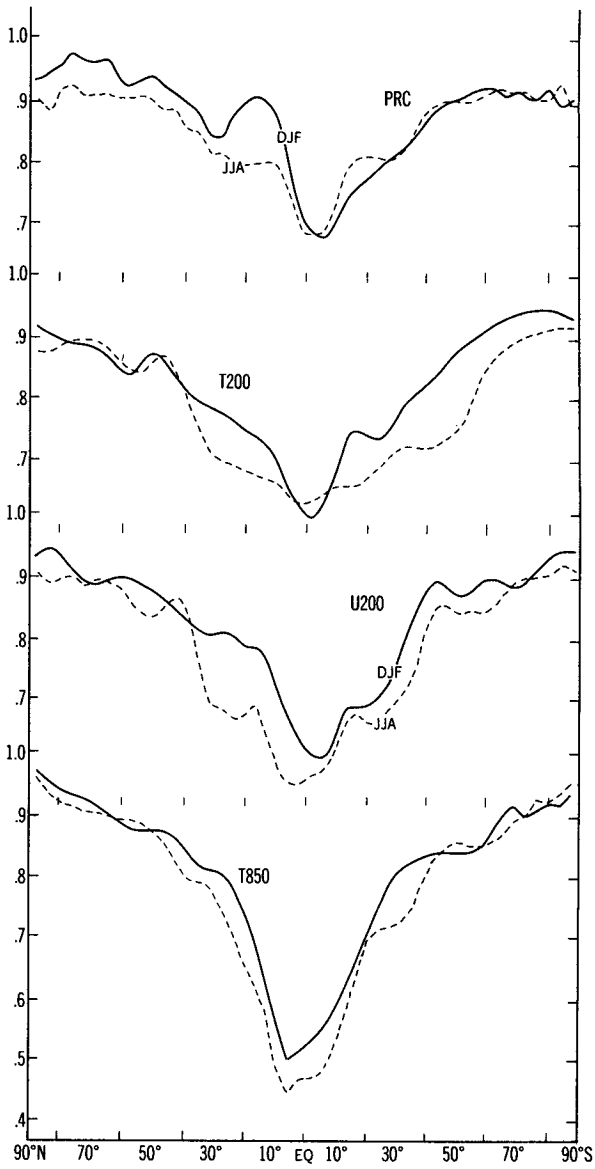

FIG. 8. Seasonal dependence of zonally averaged reproducibility, ΣR from Eq. (4.3), for four variables. The solid curves are for DJF, and the dashed curves for JJA.

In Fig. 9, which shows R for precipitation rate for both DJF and JJA, one can see the tendency for improved reproducibility to extend toward the extratropics, more in JJA than DJF, this tendency is even more evident for Z500 (Fig. 10). However, for precipitation rate, this does not happen everywhere. For example, in the North American sector, a region of greater reproducibility stands out across the southeast United States in DJF, which is possibly associated with the wintertime subtropical jet position.

c. *Reproducibility in the T42 model*

To enhance the credibility of the discussions that follow, the results from a second group of simulations,

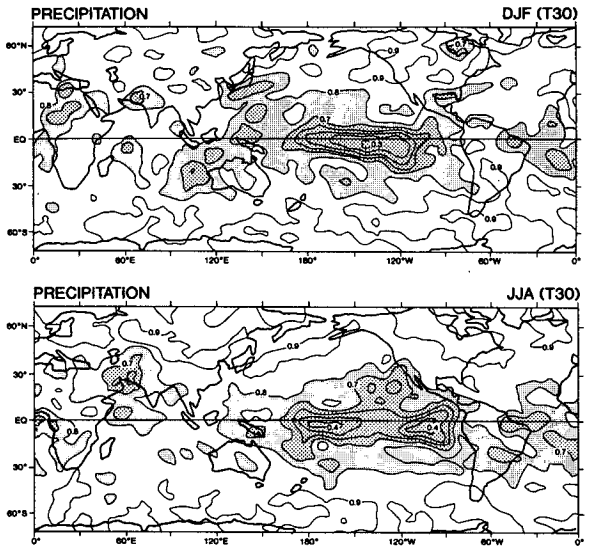

FIG. 9. Global distribution of reproducibility, σ_R/σ_S, for the precipitation rate during DJF (upper), and that during JJA (lower). Contour interval is 0.1. The regions of <0.8 are indicated with small stipples and those of <0.7 are indicated with larger stipples.

run with a T42L18 version of the model ("T42SM," as described in section 2), will sometimes be presented along with those from the T30SM.

Figure 11 shows the time-averaged, DJF and JJA, reproducibility of precipitation rate for the T42SM ensemble. These geographically distributed reproducibilities may be compared to those of the T30SM (Fig. 9). It is reassuring to see that the reproducibility pattern of the T42SM generally confirms that of the T30SM. This is quite evident in the equatorial regions, but there is also a significant degree of agreement in those areas where better reproducibility extends to higher latitudes. The T42SM appears to have a somewhat greater extent of low values of R than the T30SM, which appears to be associated with slightly larger values of seasonal variability—that is, σ_S—but the differences here may not be significant. It appears that the U.S. region has R values averaging about 0.85, which is significantly greater than the highly reproducible and predictable east equatorial Pacific. Reproducibility values over the U.S. region are somewhat improved by calculating R for model soil moisture (not shown) instead of precipitation.

5. Reproducibility and seasonal prediction

a. Reproducibility in time series

A goal of seasonal prediction is to use the ensemble prediction approach to derive an a priori measure of confidence of the ensemble mean prediction. In the study here it has been proposed that reproducibility may be one such measure. If this is the case it seems reasonable to expect that model predictions should show more skill more often when reproducibility is better (lower R values) than when R values are high.

Another goal (or wish) is to be able to forecast those significantly anomalous situations, such as droughts, extended periods of excessive wetness, extended cold waves, etc. In this regard, outside of the Tropics, it seems reasonable to look at the U.S. region (Fig. 5, boxes 3 and 4), given the occurrence of at least a few such extreme events during the decade of interest here

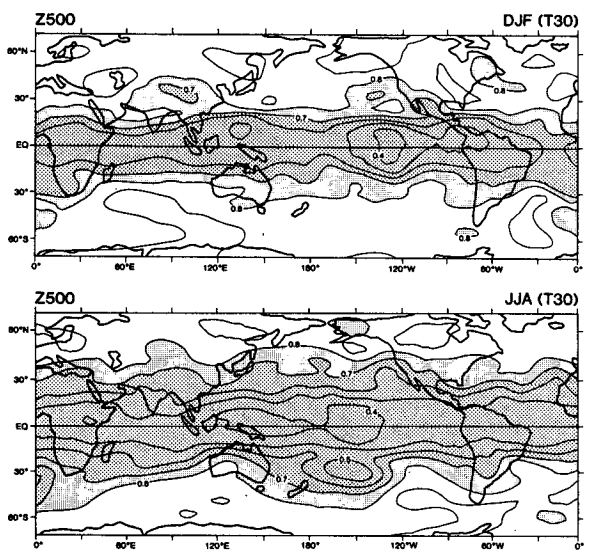

FIG. 10. Global distribution of reproducibility, σ_R/σ_S, for geopotential height at 500 hPa during DJF (upper), and that during JJA (lower). Contour interval and stippling patterns are the same as in Fig. 9.

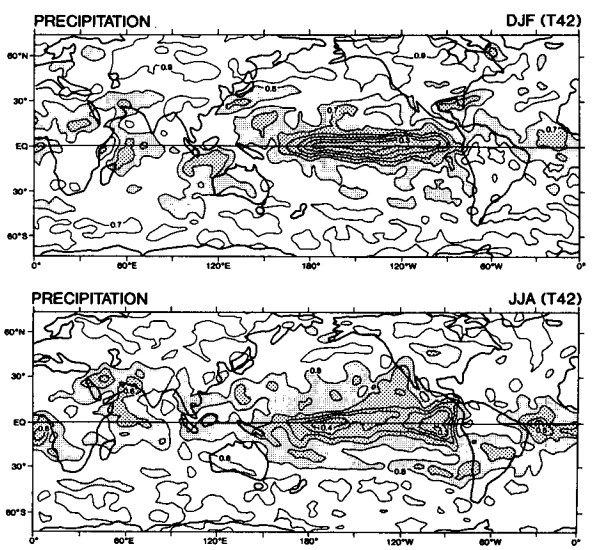

FIG. 11. Global distribution of reproducibility, σ_R/σ_S, for the precipitation rate in the T42SM, during DJF (upper) and JJA (lower). Contouring and stippling are the same as in Fig. 9.

and the availability of observed validation data. An encouraging factor is evidence of a good statistical relationship between SST anomalies in the eastern equatorial Pacific and an atmospheric mode similar to the PNA (Lau and Nath 1994; Wallace and Gutzler 1981). Being immediately downstream, weather regimes across the U.S. region should be influenced by the strength of the PNA.

If one examines the time series behavior of reproducibility, significant swings are evident as seen in Fig. 12 for the T30SM simulations. The top panel of Fig. 12 displays the 3-month running mean of soil moisture (Sm) in boxes 3 and 4 combined. The ensemble mean of nine members is shown by the thick line, which is (dropping subscript notation) $\langle x' \rangle$, calculated based on (3.1). At any arbitrary point in time (along the abscissa of this diagram), the values from the solutions of each of the nine ensemble members are taken and the standard deviation of Sm is calculated—that is, σ_n, based on (4.1). This is the "spread," which is shown by the thick solid line in the middle panel of Fig. 12. On the other hand, the seasonal variability of the spread is calculated as the variation over a decade—that is, σ_s, based on (3.4)—which is depicted by the thin dashed line in the middle panel. The cyclic variation of the curve is simply the repetition of the same variation every year. This panel also indicates that the spread exhibits considerable interannual variability, sometimes small, and other times large. To examine the seasonally adjusted spread, the reproducibility is calculated by Eq. (4.2)—that is, $R = \sigma_n/\sigma_s$. This is the normalized spread or the reproducibility.

The implications of this bottom curve are most crucial to the goal of this paper. To the extent that the low values of R (good reproducibility) are significant, it suggests that the ensemble mean anomalies, $\langle x' \rangle$, have real variability in time; that is, as N becomes large $\langle x' \rangle$ should not tend toward zero, as might be expected in a truly chaotic system. In this regard, it is suggested here that R may be capable of providing some measure of potential predictability as a function of time (and space); however, there is some concern in determining significance.

b. *Model simulations of droughts and moisture excesses*

In this subsection the focus will be on assessing the performance of the model in simulating excessive dryness and wetness as seen in seasonal anomalies. Specifically, predictions of soil moisture and precipitation rate anomalies will be presented.

It is intriguing to look at soil moisture as a field relevant to seasonal prediction. By definition it has "memory" since it has a storage capacity. This integral effect should help to filter out "noise." Furthermore, accurate soil moisture prediction on a seasonal timescale would be quite useful for agricultural interests, especially in the summer.

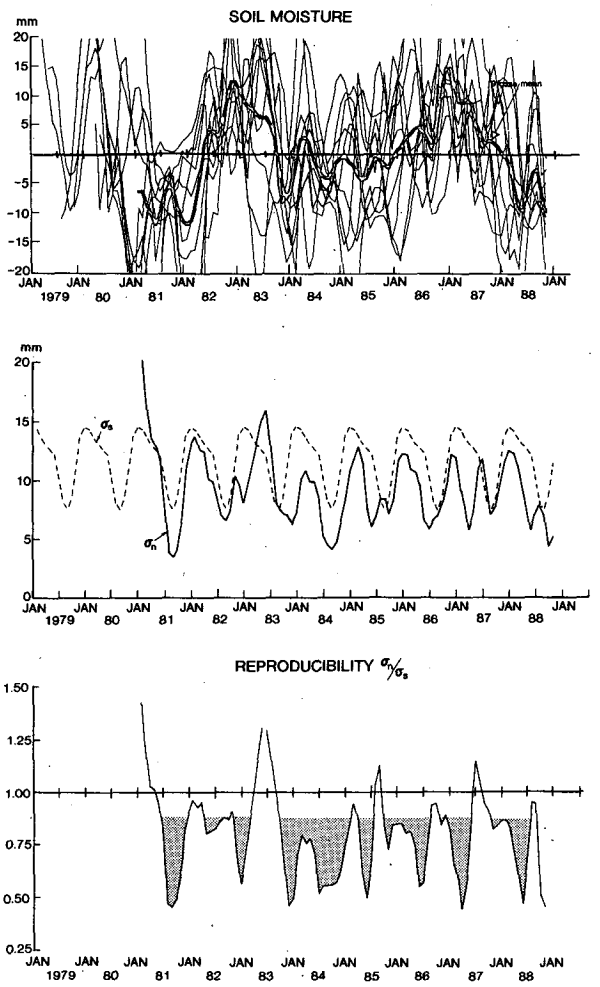

FIG. 12. Time series of the spread of soil moisture for the United States (combination of boxes 3 and 4). The nine individual anomaly solutions are shown as solid lines and the ensemble mean is indicated with a thick bold line (top), the ensemble spread is plotted with a solid line and the seasonal variability indicated with a thin dashed line (middle), and the normalized spread (bottom).

From any perspective, model validation of soil moisture presents some difficulties, as it is not an easy quantity to directly measure. Indirect assessments of soil moisture or closely related quantities are available, however. The Palmer Hydrological Drought Index (PHDI) is used here as a qualitative measure for validating the model soil moisture fields in the U.S. region. It is one of a number of drought indices designed by Palmer (1965) using the principles of balance between moisture supply and demand (see also Karl 1983; Rind et al. 1990) and was chosen here because of its longer timescale (not subject to short timescale precipitation events) than some of the other indices. Figure 13 shows the PHDI averaged over the United States for the period of concern here (1980 to 1988). This plot clearly depicts two drought periods, the first involves two summers extending from the summer (JJA) of 1980

through the summer of 1981 and the second is for the spring through summer of 1988, and periods of excessive wetness starting near the winter of 1982/83 and generally remaining wet through the winter of 1986/87.

A second indirect "observed" measure of soil moisture used here was processed by Schemm et al. (1992) following a procedure derived by Mintz and Serafini (1984) and based on the method proposed by Thornthwaite (1948; see appendix). It uses observed monthly mean precipitation and estimated potential evapotranspiration, based on surface air temperature, to compute changes in soil moisture. The advantage of using this dataset (hereafter referred to as NASA_Sm) is that it is available as gridded analyses and so can be easily compared over the same U.S. region as was defined for the model—that is, boxes 3 and 4 (see Fig. 5). Figure 14 compares the NASA_Sm (solid line) with the simulations the T30SM (dotted line) and the T42SM (dashed line). There appears to be some agreement between the model simulations and the NASA_Sm, with overall correlations (with the NASA_Sm) of 0.47 and 0.25 for the T30SM and T42SM, respectively. The agreement is good for the major droughts of 1981 and summer of 1988 and the excessive wetness associated with the 1982/83 winter; however, the T42SM verifies rather poorly for 1987 into the spring of 1988 relative to the T30SM performance. The poorer performance of the T42SM may not be significant, but in any case, it should be noted that SST datasets were different for the T42SM versus the T30SM (see section 2).

Verification of precipitation over the U.S. Region is not nearly as good as was seen for soil moisture, with correlations of less than 0.15 for both the T30SM and the T42SM, using observed precipitation data obtained from the Goddard Space Flight Center (see Schemm et al. 1992) (hereafter referred to as NASA_Pr). This result is somewhat expected based on the earlier discussion of reproducibility values for precipitation rate and soil moisture.

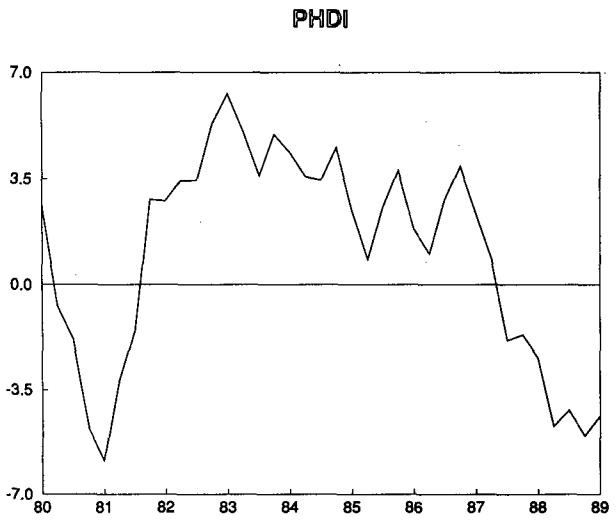

FIG. 13. Time series of observed PHDI averaged over the entire United States.

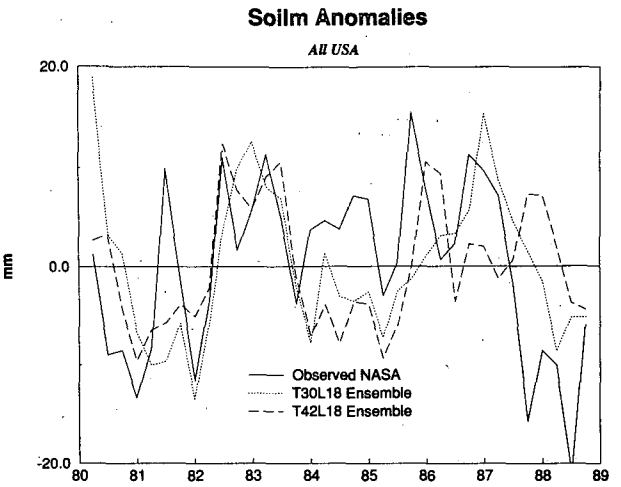

FIG. 14. Time series of ensemble mean soil moisture anomalies averaged over the combined region of boxes 3 and 4 for the T30SM ensemble (dotted line), T42SM ensemble (dashed line), and estimated observations (solid line) from Schemm et al. (1992).

To further explore a possible connection between good reproducibility and good predictive skill in the model extratropics, one can focus the validation more precisely on an area that appears to have good reproducibility. In the top panel of Fig. 9 (DJF) it can be seen that the southeastern United States stands out in the extratropics as having good reproducibility (i.e., R values of about 0.8 or less). The association of observed precipitation near the Gulf Coast and in the southeastern United States with the Southern Oscillation (SO) during November–March was pointed out by Ropelewski and Halpert (1986), with the highest potential predictability of rainfall found for those regions (together with the Ohio Valley) in February–April by Richman et al. (1991) (see also Livezey 1990). For validation purposes a special southeast U.S. region is defined from 105° to 70°W long and between 25° and 35°N lat. Figure 15 shows a comparison of precipitation rate anomalies for the southeast U.S. region using the NASA_Pr validation data. The overall performance here is noticeably better than for more general U.S. region (boxes 3 and 4) shown above, with correlations of 0.32 and 0.38 for the T30SM and T42SM, respectively. Specifically, there is particularly good agreement for the drier than normal winters of 1981, 1985, and 1988 (La Niña years), the wet winters of 1982/83, and also to some extent for 1986/87 (El Niño years). This appears to offer some additional encouraging evidence for using reproducibility as an indication of predictability. It also suggests that perhaps periods

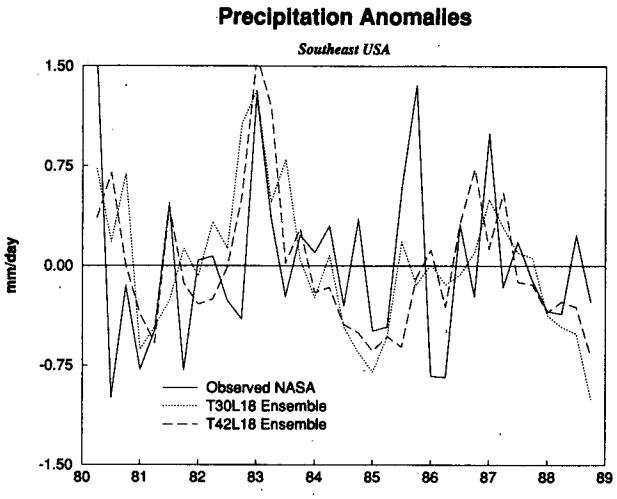

FIG. 15. Same as Fig. 14 except for precipitation rate over the southeast U.S. region.

in which reproducibility is not good should be excluded from verification.

As a final example to support the hypothesis that good reproducibility is associated with greater predictability, precipitation rate is validated for the northeast Brazil region as shown in Fig. 16. This is a tropical region of particular interest for prediction on seasonal timescales (Ward et al. 1988). Good reproducibility in a time-averaged sense was apparent for both DJF and JJA from Fig. 9. It is also quite evident in Fig. 16 that there is significant predictive skill for precipitation, with an overall correlation of 0.59.

6. Conclusions and comments

Decadal timescale simulations of the atmosphere have been performed, using a spectral GCM at resolutions of T30 and T42 (T30SM and T42SM), prescribing the lower boundary from datasets of ocean surface temperatures. The global ocean surface temperatures, based on observations of Reynolds (1988) and AMIP (Gates 1992), varied in time for the decade (1979–1988). Based on an ensemble size of nine, a series of investigations were performed with the ultimate goal of assessing the feasibility of seasonal prediction.

The general circulation statistics presented for the T30SM in section 3 look realistic; however, several significant drawbacks have been indicated. Deficiencies in the Walker Circulation are characterized by westerly errors in the upper-tropospheric equatorial Pacific, upper-tropospheric easterly errors near India, and surface easterlies that are too weak over New Guinea and Borneo. These errors are likely related to the very excessive precipitation that occurs in the western tropical Pacific, especially during JJA.

Spread among ensemble members was discussed in section 4 and a measure of this spread, reproducibility (R), was defined. It was shown that the best reproducibility occurs in the equatorial regions, especially over the Pacific, and becomes poorer moving toward the higher latitudes. Yet, there are some regions of good reproducibility that occur in the extratropics, one such area being the southeast United States in DJF.

Geographical distributions of precipitation rate reproducibility in the T42SM confirms those of the T30SM. Time series verification of model results hints of predictive skill for soil moisture anomalies, particularly for the 1981 and 1988 droughts and the excessive wetness of 1983; these are also periods of good reproducibility. Precipitation validation for the U.S. region does not show predictive skill, except in the southeast United States, where there is better reproducibility in a time average sense.

An example of good reproducibility corresponding with predictability was shown by validating precipitation rate in the Northeast Brazil region.

a. *Summary*

- The T30SM model used in this study performs reasonably well. However, there are several significant biases, for example, along the SPCZ and the ITCZ, there is excessive precipitation at the western and central equatorial Pacific in DJF and near the Philippines in JJA.
- The high consistency and reproducibility of the ensemble of simulations in the Tropics relative to the extratropics seems to be indicating greater predictability in the Tropics assuming that the global SST distribution is known.
- Multiple simulations appear necessary for seasonal prediction in the extratropics. Outside of the Tropics, good reproducibility appears to be regional and a function of time; this implies *that there may be occasional predictable periods in the extratropics,* which probably

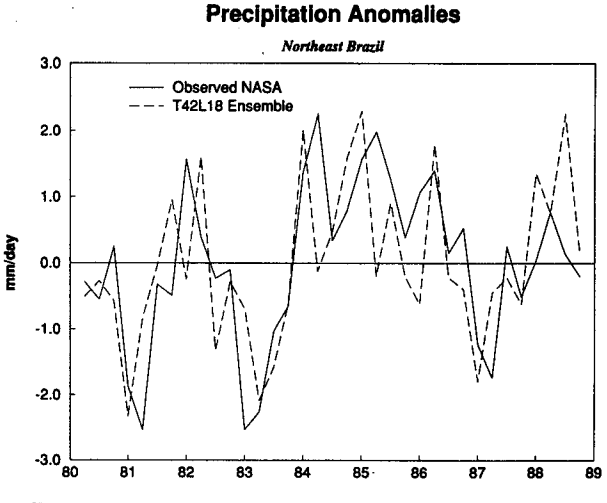

FIG. 16. Same as Fig. 15 except for Northeast Brazil region.

depend on SST distributions and possibly their evolution in time as well. One needs the information from an ensemble of solutions to make a priori determination of reproducibility (and possibly predictability) as a function of time.

- Soil moisture in the initial condition should be specified carefully. In simulations over extended periods of time, it is determined by the evolution of SST and the physics of the GCM (see appendix).
- It is speculated that some moisture extremes over the United States, particularly droughts, might be predictable, if SST is known. But future work is necessary before a more definitive determination can be made.

b. *Comments*

This study was based on the uncoupled model. The presence of systematic forcing, external to the atmosphere, appears crucial for predictive skill on these timescales. However, the true memory system should be contained in the coupled system. In this sense, the discussions in this paper represents a partial story regarding predictability.

The objective of this paper is to present the concept of reproducibility and how it might be indicative of seasonal predictability. In this study it is implied that seasonal predictability is associated with reproducibility of seasonal anomalies; however, this may be too limiting. One should be open to a broader view of seasonal predictability. For example, forecasts of expected changes in atmospheric circulation variability on a seasonal timescale may provide useful information.

Finally, a question remains as to what extent ensemble mean anomaly and reproducibility patterns are robust irrespective of the GCM. In this regard, the ongoing AMIP project (Gates 1992) may be enlightening.

Acknowledgments. The authors would like to thank Dr. John Lanzante, Mr. Richard Heim, Mr. Anthony Rosati, and Dr. Robert Livezey for their helpful discussions and feedback. We would also like to thank Mr. Robert Smith for processing and analyzing much of the data, as well as, Mr. Richard Gudgel for his help with some of the analyses and Dr. A. Kitoh for providing us with several figures of their GCM results. In addition, we appreciate the helpful reviews provided by Drs. N. C. Lau, J. Anderson, T. N. Palmer, and an anonymous reviewer. Finally, we extend our thanks to the GFDL illustration group for skillfully drafting most of the figures.

APPENDIX

Soil Moisture in Initial Conditions

Soil moisture is not an entirely independent quantity. In this study, it is specified within the context of the "bucket method" (Manabe 1969). Yet the discussion in this appendix may be valid for other ground hydrology techniques as well.

During the first year of the simulations, there is a period in which the adjustment of the soil moisture takes place. This adjustment is seen rather clearly in Fig. A1. Three surface variables—the precipitation, the ground temperature, and the soil moisture—vary similarly in time for most of the 10 years, except during the first year. The reason why this spinup occurred is that the soil moisture at the initial time was not in "hydrological balance" with the other variables. Initial soil moisture was taken from the climatological values of ECMWF analyses and it was not initialized within the framework of the T30SM model.

It is somewhat surprising to learn that the adjustment is such a slow process; more than one season and sometimes up to about 1 year is required for the soil moisture to reach its equilibrium. Figures A2 and A3 exhibit the behavior of this variable in two regions—that is, box 4 (from Fig. 5, the eastern United States) and for a portion of Asia, respectively. Three curves of soil moisture are included in these figures. The first is the solution in one of the nine simulations. The second and the third are the climatological annual cycle of the ECMWF, and of the T30SM model.

The diagrams illustrate that the value of soil moisture in the simulation starts from that of the ECMWF climatology and then converges steadily to the T30SM climatology. It is apparent that the climatological seasonal cycles for soil moisture from the ECMWF analysis/model and the T30SM differ appreciably from one another, and there is no objective yardstick at present to assess the "correctness" of the hydrology schemes. In this respect, it is worthy to note that Wolfson et al. (1987) and Atlas et al.

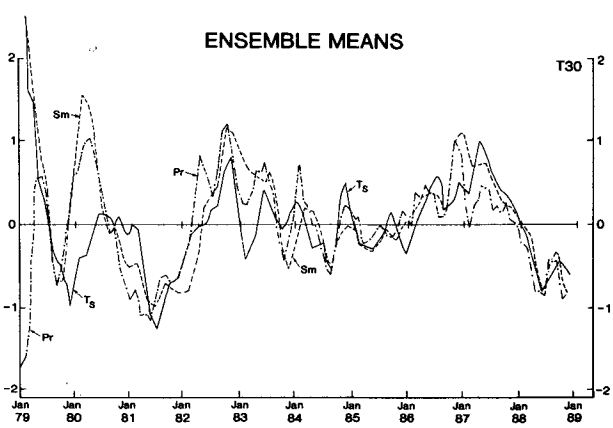

FIG. A1. Plots of the ensemble mean anomalies for precipitation rate, soil moisture, and surface temperature. All variables are normalized, and the vertical scale for temperature is reversed.

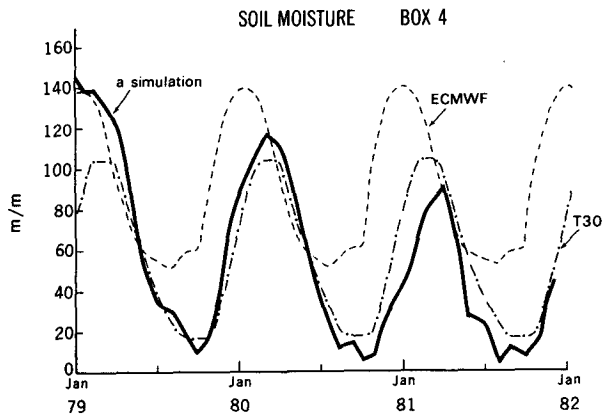

FIG. A2. Time variation of the soil moisture in box 4 (eastern United States). One simulation from the T30SM ensemble (thick bold line), the ECMWF climatological seasonal cycle (dotted line), and the T30SM climatological seasonal cycle (dashed dotted line).

(1995) have devised schemes to determine the soil moisture boundary condition. They make use of Mintz and Serafini's (1984) procedure to derive soil moisture by applying the observed surface air temperature and precipitation. Presumably, a corresponding data assimilation approach in which observed precipitation is inserted could be used to calculate soil moisture.

To summarize, it is suggested that (a) the soil moisture in GCMs is a somewhat artificial variable, which is specified by the particular scheme of ground hydrology; (b) the values are also influenced by the cumulus convection, the boundary layer processes, etc.; (c) accordingly, initialization of soil moisture is important in order to start monthly or single season predictions (as it may take up to about one year in some cases to achieve a reasonable degree of adjustment); and (d) an arbitrary value should not be specified as an initial condition, because adjustment starts to take place immediately, if the initial state is not in hydrologic balance.

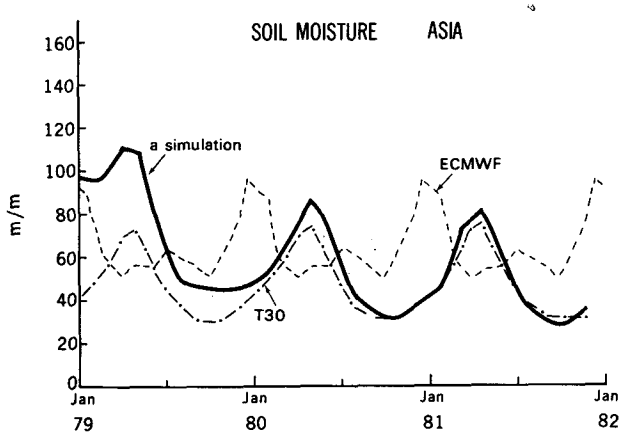

FIG. A3. The same as Fig. A2 but for a region in Asia.

REFERENCES

Atlas, R. M., N. Wolfson, and J. Terry, 1993: The effect of SST and soil moisture anomalies on the 1988 U.S. summer drought. *J. Climate,* **6,** 2034–2048.

Gates, W. L., 1992: An AMS continuing series: Global change, AMIP: The atmospheric model intercomparison project. *Bull. Amer. Meteor. Soc.,* **73,** 1962–1970.

Gordon, C. T., 1992: Comparison of 30 day integrations with and without cloud-radiation interaction. *Mon. Wea. Rev.,* **120,** 1244–1277.

——, and W. F. Stern, 1974: Spectral modelling at GFDL. The GARP Programme on Numerical Experimentation. *Int. Symp. on Spectral Methods in Numerical Weather Prediction,* Copenhagen, Denmark, WMO, 46–80.

——, and ——, 1982: A description of the GFDL global spectral model. *Mon. Wea. Rev.,* **110,** 625–644.

Horel, J. D., and J. M. Wallace, 1981: Planetary scale atmospheric phenomena associated with the Southern Oscillation. *Mon. Wea. Rev.,* **109,** 813–829.

Hoskins, B. J., and D. Karoly, 1981: The steady linear response of a spherical atmosphere to thermal and orographic forcing. *J. Atmos. Sci.,* **38,** 1179–1196.

Karl, T. R., 1983: Some special characteristics of drought duration in the United States. *J. Climate Appl. Meteor.,* **22,** 1356–1366.

Kitoh, A., 1991a: Interannual variations in an atmospheric GCM forced by the 1970–1989 SST. Part I: Response of the tropical atmosphere. *J. Meteor. Soc. Japan,* **69,** 251–269.

——, 1991b: Interannual variations in an atmospheric GCM forced by the 1970–1989 SST. Part II: Low-frequency variability of the wintertime Northern Hemisphere extratropics. *J. Meteor. Soc. Japan,* **69,** 271–291.

König, W., and E. Kirk, 1991: Interannual circulation regime fluctuations and their effect on interseasonal variability. Studying Climate with the Atmospheric Model ECHAM. Meteor. Inst. Large Scale Atmos. Modelling, Report No. 9, 115–132.

Kushnir, Y., and N.-C. Lau, 1992: The general circulation model response to a North Pacific SST anomaly: Dependence on time scale and pattern polarity. *J. Climate,* **5,** 271–283.

Latif, M., J. Biercamp, H. von Storch, M. J. McPhaden, and E. Kirk, 1990: Simulation of ENSO related surface wind anomalies with an atmospheric GCM forced by observed SST. *J. Climate,* **3,** 509–521.

Lau, N.-C., 1985: Modeling the seasonal dependence of the atmospheric response to observed El Niños in 1962–75. *Mon. Wea. Rev.,* **113,** 1970–1996.

——, and M. J. Nath, 1990: A general circulation model study of the atmospheric response to extratropical SST anomalies observed in 1950–79. *J. Climate,* **3,** 965–989.

——, and ——, 1994: A modeling study of the relative roles of tropical and extratropical SST anomalies in the variability of the global atmosphere–ocean system. *J. Climate,* **7,** 1184–1207.

Legates, D. R., and C. J. Willmott, 1990: Mean seasonal and spatial variability in gauge-corrected global precipitation. *Int. J. Climatol.,* **10,** 111–127.

Livezey, R. E., 1990: Variability of skill of long-range forecasts and implications for their use and value. *Bull. Amer. Meteor. Soc.,* **71,** 300–309.

Lorenz, E. N., 1963: Deterministic nonperiodic flow. *J. Atmos. Sci.,* **20,** 130–141.

Manabe, S., 1969: Climate and ocean circulation. Part I: The atmospheric circulation and the hydrology of the earth's surface. *Mon. Wea. Rev.,* **97,** 739–774.

Mintz, Y., and Y. Serafini, 1984: Global fields of monthly normal soil moisture as derived from observed precipitation and an estimate potential evapotranspiration. Final scientific report under NASA Grant NAS 5-26, Part V, Dept. of Meteorology, University of Maryland, College Park, MD.

Miyakoda, K., T. Gordon, R. Caverly, W. Stern, J. Sirutis, and W. Bourke, 1983: Simulation of a blocking event in January 1977. *Mon. Wea. Rev.*, **111,** 846–869.

——, A. Rosati, and R. Gudgel, 1993: Toward GCM El Niño simulation. NATO ASI Series, Vol. 16, Springer-Verlag, 125–151.

Möller, F., 1951: Viertel Jahrskarten des Niederschlags für die ganze Erde. *Petermanns Geographische Miteilungen,* Justus Perthes, 1–7.

Namias, J., 1986: Autobiography. *Namias Symp.,* La Jolla, CA, Scripps Institut. Oceanogr., Reference Series 86-17, 1–59.

Navarra, A., and K. Miyakoda, 1988: Anomaly general circulation models. *J. Atmos. Sci.,* **45,** 1509–1530.

——, W. F. Stern, and K. Miyakoda, 1994: Reduction of the Gibbs oscillation in spectral model simulations. *J. Climate,* **7,** 1169–1183.

Palmer, T. N., 1993: Extended-range atmospheric prediction and the Lorenz model. *Bul. Amer. Meteor. Soc.,* **74,** 49–65.

Palmer, W. C., 1965: Meteorological drought. Research Paper No. 45, U.S. Weather Bureau, Washington, DC, 58 pp. [Available from Library and Information Services Division, NOAA, Washington, DC 20852.]

Pitcher, E. J., M. L. Blackmon, G. T. Bates, and S. Munoz, 1988: The effect of general circulation model. *J. Atmos. Sci.,* **45,** 173–188.

Ponater, M., and W. König, 1991: Interannual circulation regime fluctuations and their effect on intraseasonal variability. Studying Climate with the Atmos. Model ECHAM, Meteor. Instit. Large Scale Atmos. Modelling, Report No. 9, 133–162.

Rasmusson, E., and T. Carpenter, 1982: Variations in tropical sea surface temperature and surface wind fields associated with the Southern Oscillation/El Niño. *Mon. Wea. Rev.,* **110,** 354–384.

Reynolds, R. W., 1988: Real-time sea surface temperature analysis. *J. Climate,* **1,** 75–86.

Richman, M. B., P. J. Lamb, and J. R. Angel, 1991: Relationships between monthly precipitation over central and eastern North America and the Southern Oscillation. *Proc., 15th Annual Climate Diagnostics Workshop,* Washington, D.C., U.S. Dept. of Commerce, 373–383.

Rind, D., R. Goldberg, J. Hansen, C. Rosenzweig, and R. Ruedy, 1990: Potential evapotranspiration and the likelihood of future drought. *J. Geophys. Res.,* **95,** 9983–10 004.

Ropelewski, C. F., and M. S. Halpert, 1986: North American precipitation and temperature patterns associated with the El Niño/Southern Oscillation (ENSO). *Mon. Wea. Rev.,* **114,** 2352–2362.

Rowntree, P. R., 1972: The influence of tropical east Pacific Ocean temperatures on the atmosphere. *Quart. J. Roy. Meteor. Soc.,* **98,** 290–321.

Schemm, J., S. Schubert, J. Terry, and S. Bloom, 1992: Estimates of monthly mean soil moisture for 1979–1989. NASA Tech. Memo. 104571, Goddard Space Flight Center, Greenbelt, MD, 252 pp.

Schubert, S., C.-K. Park, W. Higgins, S. Moorthi, and M. Suarez, 1990: An atlas of ECMWF analysis (1980–87). Part I: First moment quantities. NASA Tech. Memo. 100747, Goddard Space Flight Center, Greenbelt, MD, 258 pp.

Shukla, J., 1985: Predictability. *Advances in Geophysics,* Vol. 28B, Pergamon, 87–122.

Simmons, A. J., J. M. A. Wallace, and G. W. Branstator, 1983: Barotropic wave propagation and instability, and atmospheric teleconnection patterns. *J. Atmos. Sci.,* **40,** 1363–1392.

Sirutis, J., and K. Miyakoda, 1990: Subgrid scale physics in 1-month forecasts. Part I: Experiment with four parameterization packages. *Mon. Wea. Rev.,* **118,** 1043–1064.

Stern, W. F., and R. T. Pierrehumbert, 1988: The impact of an orographic gravity wave drag parameterization on extended range predictions with a GCM. *Proc. Eighth Conf. on Numerical Weather Prediction,* Baltimore, MD, Amer. Meteor. Soc., 745–750.

——, and K. Miyakoda, 1989: Systematic errors in GFDL's extended range prediction spectral GCM. *Proc. Workshop on Systematic Errors in Models of the Atmosphere,* Toronto, Canada, WMO, TD No. 273, 136–140.

——, and ——, 1991: The feasibility of seasonal NWP from decadal simulations. *Proc. Ninth Conf. on Numerical Weather Prediction,* Denver, CO, Amer. Meteor. Soc., 649–651.

Thornthwaite, C. W., 1948: An approach toward a rational classification of climate. *Geophys. Rev.,* **38,** 55–94.

Tiedtke, M., 1986: Parameterization of cumulus convection in large scale models. *Physically-Based Modeling and Simulation of Climate and Climate Change,* M. E. Schlesinger, Ed., Reidel, 375–431.

Ting, M., and I. M. Held, 1990: The stationary wave response to a tropical SST anomaly in a idealized GCM. *J. Atmos. Sci.,* **47,** 2546–2566.

Trenberth, K. E., and G. W. Branstator, 1992: Issues in establishing causes of the 1988 drought over North America. *J. Climate,* **5,** 159–172.

——, ——, and P. A. Arkin, 1988: Origins of the 1988 North American drought. *Science,* **242,** 1640–1645.

Troup, S., 1967: Opposition of anomalies in upper tropospheric winds at Singapore and Canton Island. *Aust. Meteor. Mag.,* **15,** 32–37.

van Loon, H., and J. C. Rogers, 1981: The Southern Oscillation. Part II: Associations with changes in the middle troposphere in northern winter. *Mon. Wea. Rev.,* **109,** 1163–1168.

Vukicevic, T., 1991: Nonlinear and linear evolution of initial forecast errors. *Mon. Wea. Rev.,* **119,** 1602–1611.

Wallace, M. J., and D. S. Gutzler, 1981: Teleconnections in the geopotential height field during the Northern Hemisphere winter. *Mon. Wea. Rev.,* **109,** 784–812.

Ward, N., C. K. Folland, and S. Brooks, 1988: Predictability of seasonal rainfall in the Nordeste region of Brazil. *Recent Climate Change—a Regional Approach.* S. Gregory, Ed., Belhaven Press, 237–251.

Wolfson, N., R. M. Atlas, and Y. C. Sud, 1987: Numerical experiments related to the 1980 heat wave. *Mon. Wea. Rev.,* **115,** 1345–1357.